Possible dominance of the Maki–Thompson process in the fluctuation conductivity of Bi-2212 superconducting whiskers

2006 J. Phys.: Condens. Matter 18 8295

(http://iopscience.iop.org/0953-8984/18/35/015)

INSTITUTE OF PHYSICS PUBLISHING JOURNAL OF PHYSICS: CONDENSED MATTER

J. Phys.: Condens. Matter **18** (2006) 8295–8312 doi:10.1088/0953-8984/18/35/015

Possible dominance of the Maki–Thompson process in the fluctuation conductivity of Bi-2212 superconducting whiskers

M Truccato[1], A Agostino[2], G Rinaudo[1], S Cagliero[1] and M Panetta[2]

[1] Dipartimento di Fisica Sperimentale, NIS-Centre of excellence and CNISM UdR Torino Università-Via P Giuria 1, I-10125, Torino, Italy
[2] Dipartimento di Chimica Generale ed Organica Applicata, NIS-Centre of Excellence and CNISM UdR Torino Università - C.^{so} Massimo D'Azeglio 48, I-10125, Torino, Italy

E-mail: truccato@to.infn.it

Received 28 January 2006, in final form 10 July 2006
Published 18 August 2006
Online at stacks.iop.org/JPhysCM/18/8295

Abstract

We report the measurement of the a-axis fluctuation conductivity in zero field for $Bi_2Sr_2CaCu_2O_{8+x}$ microcrystals. A complete geometrical characterization allows us to determine the absolute value of the excess conductivity and its temperature behaviour with high accuracy. A careful application of the complete fluctuation theory (Varlamov *et al* 1999 *Adv. Phys.* **48** 655), which implements a minor correction for the $\tilde{k}$ factor and a suitable procedure for disentangling the influence of the different fit parameters, shows that data interpretations excluding the Maki–Thompson (MT) process are either not consistent with the crystal structure or not self-consistent. On the other hand, a data interpretation including the MT process appears to be both self-consistent and consistent with experimental measurements of the electron dephasing time τ_ϕ performed in other metallic or semiconducting systems. According to the latter scheme, the anomalous MT term could be a very important contribution to the excess conductivity throughout the temperature range of interest and thus the s-wave symmetry becomes an important component of the order parameter above T_c.

1. Introduction

The additional contribution to the normal state conductivity due to Cooper pairs formed above T_c ($\Delta\sigma$, also called paraconductivity or excess conductivity) was theoretically investigated for the first time by Aslamazov and Larkin (AL) [1], who obtained for 2D systems $\Delta\sigma_{AL}^{2D} = e^2/(16\hbar d\varepsilon)$, where $\varepsilon = (T - T_c)/T_c$ and d is the thickness of the 2D layer. Soon after,

Maki and Thompson (MT) [2, 3] calculated two other leading contributions (one regular and one anomalous) to the paraconductivity, showing that decayed pairs can scatter on an impurity potential as though they were still paired, due to time-reversal symmetry. These contributions explained the experimental data for low T_c superconductors fairly well [4].

With the appearance of the high-T_c superconductors, it was soon recognized that thermodynamic fluctuations were responsible for the smoothing of the transition in these systems [5], but a debate arose on the role of the MT contributions, which were initially not detected. From the theoretical point of view, the importance of the layered superconductor model by Lawrence and Doniach [6] was greatly enhanced by the crystallographic structure of high-T_c superconductors. Moreover, Dorin *et al* [7] pointed out the necessity of taking into account the fact that electrons involved in fluctuating pairs cannot contribute to ordinary conductivity, therefore suppressing the quasiparticle density of states (DOS). Recently, a comprehensive model consisting of the AL, the MT and the DOS terms was formulated for the paraconductivity both in the absence and in the presence of a magnetic field, including also a slight modification in the numerical coefficient for the anomalous MT term [8, 9].

On the experimental side, the relative importance of each contribution has long been debated. The leading role of the AL contribution is presently usually accepted and the DOS term is believed to be a comparable correction whose importance decreases with increasing the sample doping or the material isotropy [10–12].

As regards the MT terms, during recent years most authors have either explained their data in a framework where the MT contributions were absent or have reported them to be unfit or negligible, both for polycrystalline [5, 13, 14] and for single crystal samples [15–22]. Also, in the experiments focused on the paraconductivity effects in a magnetic field, the MT terms have often been omitted in the data interpretation due to the fact that they were presumed to be very small or that they proved to be inconsistent with the experimental results [12, 18, 23–25]. Nevertheless, some slight evidence for the necessity of also considering these contributions in order to obtain a satisfactory explanation both of the in-field paraconductivity [26, 27] and of the NMR relaxation rate [28] measurements was already present. After the importance of the DOS term was well understood, a more careful analysis of the in-field paraconductivity data including also the DOS suppression effect could not exclude the presence of the MT process in previous experiments, therefore putting the conclusions against it back into consideration [29]. Since then, the role of the MT terms has been rediscovered and several paraconductivity experiments have been interpreted, also including these terms as essential for a quantitative agreement with the theory. Most of them have been performed in a magnetic field [10, 11, 30–33], but some also in zero field [32, 34]. All of them share the conclusion that the MT terms are only slightly important. This is expected for in-field experiments, since the MT process is believed to be strongly suppressed by the magnetic field, but it has not to be necessarily the same for the zero-field experiments, depending on the microscopic characteristics of the systems under study. Interestingly, the debate about the role of the MT process also has an implication from the point of view of the symmetry of the order parameter. In fact, among the above-mentioned contributions to the paraconductivity, these are the only ones that should vanish in case of a pure d-wave symmetry [9, 28].

The purpose of the present work is to contribute to this debate by adding accurate experimental data taken in zero field on very good microscopical $Bi_2Sr_2CaCu_2O_{8+x}$ (Bi-2212) crystals. It will be shown that, besides more traditional frameworks excluding the MT contributions, a data interpretation where the MT anomalous term is the most important one throughout the whole temperature range of validity of the fluctuation model is both possible and reasonable.

Table 1. Relevant sizes for samples WI3B_1 and WI3C_1. L is the total crystal length, Δx is the distance between midpoints of voltage contacts, W is the crystal width and t the thickness. WI3C_1(a) and WI3C_1(b) refer to the two parts in which the growth step divides the crystal longitudinally (see text).

Sample	L (μm)	Δx (μm)	W (μm)	t (μm)
WI3B_1	1486.3 ± 02.8	300 ± 3	6.35 ± 0.26	1.10 ± 0.08
WI3C_1(a)	1499 ± 23	129 ± 8	3.26 ± 0.15	0.680 ± 0.021
WI3C_1(b)			2.86 ± 0.13	0.758 ± 0.024

2. Experimental details

Our experiment was performed by using microscopic whisker-like Bi-2212 single crystals grown by the method of glassy plate oxygenation. These crystals grow with the a-axis aligned with the length direction, the b-axis in the width direction and the c-axis along the thickness. Typical crystal sizes are 1 mm in length, 10 μm in width and 1 μm in thickness and it has already been demonstrated that this kind of sample shows a considerably lower density of defects in comparison with bulk ones [35, 36].

It is well known that in Bi-2212 the oxygen diffusion occurs essentially in the ab-plane with the highest rate along the a-axis direction [37], which is also the direction with the largest crystal size, and it has also been shown that the copper ion diffusion takes place along the b-axis direction on a timescale of tens of days at ordinary environmental conditions [38]. These facts make it very likely that in freshly grown Bi-2212 whiskers the small volumes intended for the investigation of the excess conductivity (maximum size of about $300 \times 6 \times 1$ μm^3 in the present study) are homogeneous from the point of view of the oxygen doping and of the copper ion concentration.

Eleven freshly grown crystals were mounted onto sapphire substrates and silver plus gold electrodes were evaporated onto their top surfaces to obtain a chip suitable for standard four-probe resistivity measurements. The details of the sample preparation have been reported in a previous paper [39] and resulted in a typical contact resistance ≈ 2 Ω, corresponding to a specific resistance $\approx 10^{-6}$ Ω cm^2.

Since we were interested in the absolute measurement of the paraconductivity, much attention was paid to the sample geometrical characterization. All sizes in the length direction were measured by means of SEM comparisons with calibrated standards, while crystal widths and thicknesses were measured by scanning the crystal length in a series of AFM maps, each of them about 22×22 μm^2. This procedure, along with the electrical characterization, allowed us to select very regularly shaped single phase crystals for further analysis. At the end of this stage only two nearly perfect samples survived, corresponding to two slightly different (7–8 °C) growth temperatures [39]. Their sizes are reported in table 1: one sample (WI3C_1) shows a 78 nm growth step, so that its cross section corresponds to two neighbouring rectangles. It should be noted that the uncertainties in the thickness are quite large, even if care was taken to exclude the regions corresponding to some submicron droplet-like impurities located on the top of the crystals [39]. Actually, the uncertainties in the sample geometry ($\approx 10\%$) are the major sources of error for this study and a suitable procedure was developed to overcome this problem, as will be explained below.

Figure 1 shows the temperature behaviour of the resistivity along the a-axis (ρ_a) for the two samples. The resistivity was obtained by four-probe voltage measurements considering the distance between the electrode midpoints. In fact, the analytical treatment by Esposito *et al* [40] has shown that the disentanglement of the in-plane (ρ_{ab}) and out-of-plane (ρ_c) resistivity

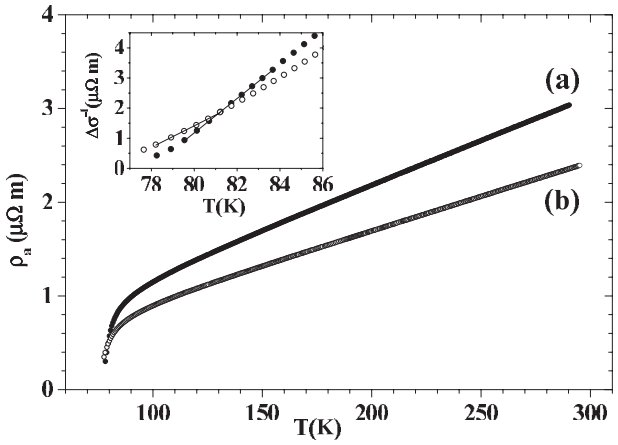

Figure 1. Temperature behaviour of the resistivity ρ_a in the a-axis direction for samples WI3B_1 (curve (a), ●) and WI3C_1 (curve (b), ○). The feeding currents were $I = 1\ \mu$A for sample WI3B_1 and $I = 2\ \mu$A for sample WI3C_1. The vertical error bars associated with each data point are not shown for clarity. The inset shows the reciprocal of the paraconductivity $\Delta\sigma$ as a function of the temperature. Solid lines in the inset represent the fits to the pure 2D AL formula.

components occurs for $L \gg \pi\sqrt{\rho_c/\rho_{ab}}\ t$, which is within our experimental range, and the corresponding relative corrections for our samples are below 4×10^{-7}, which can be neglected. The measurements were collected on sample warming in steps of 0.5 K every 130 s; no care was taken to exclude the Earth's magnetic field. The average of the readings collected in ten subsequent current reversals at the rate of ≈1 Hz was performed in order to cancel the thermal emfs, with a temperature stability for the sample of ±0.01 K during each reading cycle. A conservative estimate of the absolute voltage error gave 60 nV, corresponding to a maximum relative error of about 0.2% in the temperature range used for the paraconductivity analysis.

3. Data analysis and discussion

The first step in studying the paraconductivity $\Delta\sigma(T) = 1/\rho_a(T) - 1/\rho_a^n(T)$ is the determination of the normal resistivity $\rho_a^n(T)$, which is commonly supposed to be linear in T (see, for instance, [14, 18, 41]). The validity of this behaviour down to T_c is suggested by the relatively low value of the Debye temperature $\Theta_D \approx 255$ K for Bi-2212 [42], which implies a ratio $T_c/\Theta_D \approx 0.3$. The approximation implied by this assumption has been avoided in many experiments by measuring the in-field paraconductivity $\Delta\sigma(B, T) = 1/\rho_a(B, T) - 1/\rho_a(0, T)$ [10–12, 18, 22, 24–26, 29–33], but this is not wise when trying to investigate the importance of the MT contribution, because of its suppression induced by the magnetic field. Moreover, it has been recently reported by Kim *et al* [32] that the simple assumption of a linear T-dependence for $\rho_{ab}^n(T)$ leads to a measurement of $\Delta\sigma(T)$ which is fully compatible with the in-field data $\Delta\sigma(B, T)$ and that both of them can be accounted for by the same set of microscopic parameters.

By taking the derivative of our $\rho_a(T)$ data, no deviation from linearity was detected down to $T \approx 160$ K, below which only a downwards curvature was observable. For prudential reasons, we chose to define the normal resistivity $\rho_a^n(T)$ as the low temperature extrapolation of the best linear fit for the experimental data corresponding to $T > 210$ K. All the analyses were repeated also for linear fits down to 160 K and, consistently, no significant difference was found.

As a first approach to account for our data we used the pure 2D AL law, which gives $(\Delta\sigma_{\mathrm{AL}}^{\mathrm{2D}})^{-1} \propto (T - T_{\mathrm{c}})/T_{\mathrm{c}}$ for $T \gtrsim T_{\mathrm{c}}$. The part of the paraconductivity data corresponding to the temperature range near T_{c} is shown in the inset of figure 1 in the form of its reciprocal $\Delta\sigma^{-1}(T)$: it is apparent that the 2D AL law can explain the data in a very limited temperature range of about 4 K only for both samples. Since $(\Delta\sigma_{\mathrm{AL}}^{\mathrm{2D}})^{-1} = 0$ for $T = T_{\mathrm{c}}$, by extrapolating to zero the best fits one obtains $T_{\mathrm{c}} = 77.9 \pm 0.6$ K and $T_{\mathrm{c}} = 76.1 \pm 0.6$ K for samples WI3B_1 and WI3C_1, respectively. These results will be used in the following as a preliminary estimate of the T_{c} of each sample. One can also note that in this simple model the slope of $\Delta\sigma^{-1}(T)$ is related to the thickness d of the isolated 2D superconducting layer, so that d can be deduced from the experimental data. This results in $d = 6.7 \pm 0.6$ Å and $d = 4.1 \pm 0.4$ Å for samples WI3B_1 and WI3C_1, respectively, implying a sample-dependent thickness of the superconducting layer.

According to the more advanced thermodynamical fluctuation theory in zero field [8, 9], the paraconductivity $\Delta\sigma(T)$ consists of four different contributions:

$$\Delta\sigma = \Delta\sigma_{\mathrm{AL}} + \Delta\sigma_{\mathrm{DOS}} + \Delta\sigma_{\mathrm{MT}}^{(\mathrm{an})} + \Delta\sigma_{\mathrm{MT}}^{(\mathrm{reg})}, \tag{1}$$

where

$$\Delta\sigma_{\mathrm{AL}} = \frac{e^2}{16\hbar s}\frac{1}{\sqrt{\varepsilon\,(\varepsilon + r)}} \tag{2}$$

$$\Delta\sigma_{\mathrm{DOS}} = -\frac{e^2}{2\hbar s}k \ln\left(\frac{2}{\sqrt{\varepsilon} + \sqrt{\varepsilon + r}}\right) \tag{3}$$

$$\Delta\sigma_{\mathrm{MT}}^{(\mathrm{an})} = \frac{e^2}{4\hbar s\,(\varepsilon - \gamma_\phi)} \ln\left(\frac{\sqrt{\varepsilon} + \sqrt{\varepsilon + r}}{\sqrt{\gamma_\phi} + \sqrt{\gamma_\phi + r}}\right) \tag{4}$$

$$\Delta\sigma_{\mathrm{MT}}^{(\mathrm{reg})} = -\frac{e^2}{2\hbar s}\tilde{k} \ln\left(\frac{2}{\sqrt{\varepsilon} + \sqrt{\varepsilon + r}}\right). \tag{5}$$

Here s is the spacing of the 2D superconducting layers in the c-axis direction, $\varepsilon = \ln(T/T_{\mathrm{c}})$ is the reduced temperature, $r(T) = -2J^2\tau^2 a/\hbar^2$ is the anisotropy parameter, $\gamma_\phi(T) = -\tau a/\tau_\phi$ is the phase-breaking rate and

$$k(T) = \frac{-\psi'\left(\frac{1}{2} + \frac{\hbar}{4\pi\tau k_{\mathrm{B}}T}\right) + \frac{\hbar}{2\pi\tau k_{\mathrm{B}}T}\psi''\left(\frac{1}{2}\right)}{\pi^2 a},$$

with J as the hopping energy between neighbouring layers, τ the quasiparticle scattering time, τ_ϕ the single electron phase-breaking time, $\psi(x)$ the digamma function and a given by the equation

$$a(T) = \left[\psi\left(\frac{1}{2} + \frac{\hbar}{4\pi\tau k_{\mathrm{B}}T}\right) - \psi\left(\frac{1}{2}\right) - \frac{\hbar}{4\pi\tau k_{\mathrm{B}}T}\psi'\left(\frac{1}{2}\right)\right].$$

For $\tilde{k}$ we used the value calculated by Larkin and Varlamov in [9]:

$$\tilde{k}(T) = \frac{-\psi'\left(\frac{1}{2} + \frac{\hbar}{4\pi\tau k_{\mathrm{B}}T}\right) + \psi'\left(\frac{1}{2}\right) + \frac{\hbar}{2\pi\tau k_{\mathrm{B}}T}\psi''\left(\frac{1}{2}\right)}{\pi^2 a}.$$

The only independent parameters of the theory are s, J, τ and τ_ϕ; besides, from an experimental point of view, the effect of the variation of the T_{c} value must also be carefully examined, to take into account the broadness of the transition.

In order to achieve the numerical sensitivity necessary for the analysis with such a complex model, the identification of a proper random error with the minimum possible size is crucial. Therefore our analysis was not performed on the paraconductivity itself $\Delta\sigma(T)$,

which has a large error of about 10% almost completely due to the geometrical uncertainties and therefore temperature independent, but on the non-normalized paraconductivity $\Delta\sigma'(T) = \Delta\sigma \cdot S/(I\Delta x)$ (S is the sample cross section), which shows a random error varying between 0.5% and 1.3% in the temperature range used for the analysis. Only subsequently were the results translated to the values for $\Delta\sigma$, when necessary. It should be noted that, strictly speaking, the temperature behaviour of $\Delta\sigma'(T)$ is not exactly the same as $\Delta\sigma(T)$ because of the temperature dependences of S and Δx, which are due to the thermal expansion. However, an estimate based on the linear expansion coefficients measured in [43] gives for the relative difference between the two quantities a maximum value of 0.15% throughout the temperature range used in the analysis. Therefore it can be stated that, within our experimental accuracy, $\Delta\sigma'(T)$ retains all the information concerning the temperature behaviour of $\Delta\sigma(T)$.

For the sake of accuracy, we implemented in our analysis the general *intermediate* case of the theory, avoiding restricting ourselves to the case either of the dirty limit ($4\pi\tau k_B T/\hbar \ll 1$) or of the clean limit ($4\pi\tau k_B T/\hbar \gg 1$). This required the digamma function $\psi(x)$ to be tabulated in steps of 10^{-4} in order to guarantee fully satisfactory results.

By inspecting the paraconductivity expressions shown in equations (2)–(5), it can be noted that T_c acts as a normalization factor for the abscissa axis through the definition of ε, while s does the same for the ordinate axis, since it can be factorized in all the terms. This suggests a correlation between s and T_c, implying that a good procedure for the fits consists in fixing *a priori* these two scale factors while leaving all the other parameters free. Therefore, as a general procedure, we selected a proper temperature range of the experimental data, fixed s close to the expected values and T_c close to the estimated values, and then performed the fit to $\Delta\sigma'(T)$ determining the best fit values of the J, τ and τ_ϕ parameters, together with the corresponding minimum value of the reduced chi square $\tilde{\chi}^2$. By systematically varying s and T_c, in principle this procedure was able to obtain the contour lines of the minimum $\tilde{\chi}^2$ and of the best fit values of J, τ and τ_ϕ in the (s, T_c) plane for each sample.

The MINUIT routines were used to carry out the $\tilde{\chi}^2$ minimization by means of both the gradient and the Monte Carlo method, in order to be aware of both the local and the absolute minima in the parameter space. Actually, when two practically equivalent $\tilde{\chi}^2$ minima were present, only the one corresponding to the shortest τ_ϕ was selected for conservative reasons, so that all the fits satisfy the double criterion of both the least $\tilde{\chi}^2$ and the least τ_ϕ.

As a first attempt to account for the experimental data within the thermodynamical fluctuation theory, we tried to follow the scheme of previous experiments which excluded or neglected the presence of the MT contributions [5, 12–21, 23–25]. Therefore we tried to fit the experimental data to the truncated formula,

$$\Delta\sigma = \Delta\sigma_{AL} + \Delta\sigma_{DOS}, \tag{6}$$

while retaining the same definitions for all the other quantities, including r and k, which are valid for the general *intermediate* case. Of course, this choice implied eliminating the τ_ϕ parameter from the minimization procedure because it is involved only in the $\Delta\sigma_{MT}^{(an)}$ term.

The preliminary trials, performed with the general fitting procedure previously described, showed that in this approximation there is a very strong dependence of $\tilde{\chi}^2$ on the s values and that no reasonable value of $\tilde{\chi}^2$ was achievable neither in the $s \approx 15$ Å nor in the $s \approx 5$ Å region. Therefore, to find the s values for which a reasonable $\tilde{\chi}^2$ could be obtained, we slightly modified our standard procedure by allowing s to vary as a free parameter and performed a scanning of the T_c axis by fixing its values in the range indicated by the pure 2D AL law. The corresponding results for $\tilde{\chi}^2$ and for the s, J and τ parameters are shown in figure 2 as a function of T_c.

It is clear from figure 2 that acceptable values for $\tilde{\chi}^2$ could be found for both samples. Labelling as $\tilde{\chi}^2_{min}$ the value of the absolute minimum of $\tilde{\chi}^2$, we defined the minimum region

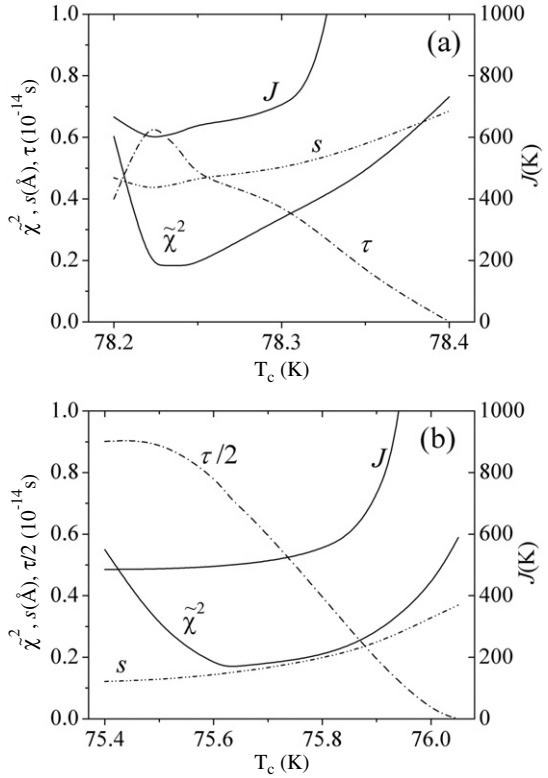

Figure 2. Behaviour of $\tilde{\chi}^2$ (——), s (— · · —), τ (— · —) and J (——) as a function of T_c for samples WI3B_1 (a) and WI3C_1 (b) obtained by fitting the experimental data to equation (6) in the general *intermediate* case. $\tilde{\chi}^2$, s and τ values are referred to the left axis, J is referred to the right axis. Panel (b) shows the values of τ divided by a factor of 2 for graphical reasons.

Table 2. Best fit parameters corresponding to the fit of experimental data of both samples to equation (6) in the general *intermediate* case. $\tilde{\chi}^2_{\rm min}$ indicates the absolute minimum of $\tilde{\chi}^2$, where $\tilde{\chi}^2 = \chi^2$ d.o.f. and d.o.f. = 10 for sample WI3B_1 and d.o.f. = 9 for sample WI3C_1 (d.o.f. stands for degrees of freedom).

Sample	T_c (K)	$\tilde{\chi}^2_{\rm min}$	s (Å)	τ (10^{-14} s)	J (K)
WI3B_1	78.26 ± 0.05	0.18	$0.47^{+0.02}_{-0.04}$	$0.46^{+0.19}_{-0.06}$	650^{+20}_{-60}
WI3C_1	75.72 ± 0.22	0.17	$0.17^{+0.07}_{-0.04}$	$1.2^{+0.6}_{-0.8}$	510^{+130}_{-20}

of $\tilde{\chi}^2$ as the T_c values where $\tilde{\chi}^2 \leqslant 2\tilde{\chi}^2_{\rm min}$. Therefore, the T_c of each sample was defined as the centre of the $\tilde{\chi}^2$ minimum region and the corresponding uncertainty was assumed as its half-width. This resulted in $T_c = 78.26 \pm 0.05$ K and $T_c = 75.72 \pm 0.22$ K for samples WI3B_1 and WI3C_1, respectively. The estimates of s, τ and J were taken as the parameter values corresponding to the T_c evaluated for each sample, while the respective uncertainties were determined as the maximum deviations from the estimated values throughout the whole uncertainty range allowed for T_c. These results are summarized in table 2.

Table 2 clarifies that, even considering their uncertainties, the best fit values of s corresponding to this approximation are completely unreasonable and have never been reported in any previous study. Also J appears to be very problematic, since, to our knowledge, only Bjornängen *et al* [31] have reported compatible values.

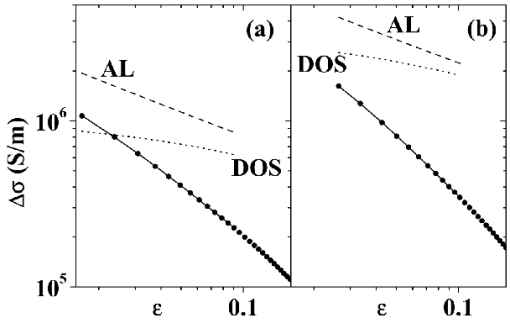

Figure 3. Best fits of experimental data to equation (6) in the general *intermediate* case for samples WI3B_1 (a) and WI3C_1 (b). Fits are represented by solid lines, single contributions by dashed and dotted lines, as indicated. The DOS term is plotted in absolute value. The corresponding parameter values are reported in table 2.

The experimental results for $\Delta\sigma$ and the best fits corresponding to the parameter values listed in table 2 are shown in figure 3. From the point of view of the experimental results, this figure shows that our data have the same qualitative behaviour already reported for Bi-2212 whiskers [44], single crystals [19, 20, 34, 41] and thin films [45], and for $YBa_2Cu_2O_{7-\delta}$ (YBCO) epitaxial thin films as well [15]. In particular, they share with previous results the order of magnitude of $\Delta\sigma$ near T_c [18, 32, 34, 41], the fact that $\Delta\sigma$ is sample dependent [5, 15, 18–20, 26, 31, 34, 41, 44] and the same dependence on the cross section already shown by Latyshev *et al* [44] in Bi-2212 whiskers. From the point of view of the data interpretation, figure 3 shows that it was possible to obtain a good fit for the experimental results to equation (6) only in somewhat limited temperature ranges ($0.017 \leqslant \varepsilon \leqslant 0.09$ for sample WI3B_1 and $0.026 \leqslant \varepsilon \leqslant 0.10$ for sample WI3C_1) and that, according to the present approximation, the DOS contribution should be significant, because it ranges from 45% to 84% of the AL term throughout the fitted temperature range for the two samples.

Even though the difficulties with the s parameter are insurmountable and led us to reject this data interpretation, it should be noted that within the framework of equation (6) the general *intermediate* case of the fluctuation theory appears to be very appropriate, since the calculation of the ratio $4\pi\tau k_B T/\hbar$ from the temperature ranges of the fits and from the τ values reported in table 2 gives $4\pi\tau k_B T/\hbar = 0.62$–$0.66$ and $4\pi\tau k_B T/\hbar = 1.53$–$1.65$ for sample WI3B_1 and sample WI3C_1, respectively.

In order to seek for further comparison between our results and previous studies, we subsequently tried to fit our experimental data to the truncated formula of equation (6) in the *clean limit* case, which implies changing the general definitions of r and k for the *intermediate* case into

$$r(T) = \frac{7\zeta(3)J^2}{8\pi^2(k_B T)^2} \qquad \text{and} \tag{7}$$

$$k(T) = \frac{8\pi^2(\tau k_B T)^2}{7\zeta(3)\hbar^2}, \tag{8}$$

respectively, where $\zeta(x)$ is the Riemann zeta function. It is worth stressing that this limit would require the condition $4\pi\tau k_B T/\hbar \gg 1$ to be fulfilled, which is not the case of our experimental data, since $4\pi\tau k_B T/\hbar = 1.65$ as an upper limit. Nevertheless, such an unwarranted assumption could shed some light on the role played by the different approximations of the theory and therefore has been pursued by using exactly the same absolute temperature T ranges and the

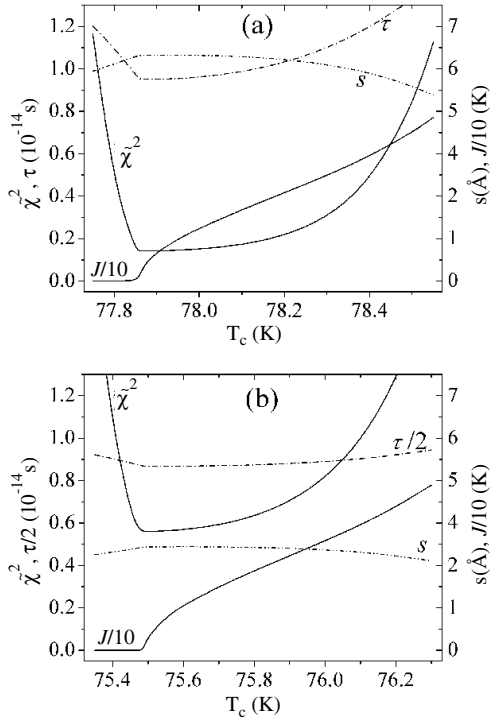

Figure 4. Behaviour of $\tilde{\chi}^2$ (——), s (— · · —), τ (— · —) and J (——) as a function of T_c for samples WI3B_1 (a) and WI3C_1 (b) obtained by fitting the experimental data to equation (6) in the *clean limit* case. $\tilde{\chi}^2$ and τ values are referred to the left axis, s and J are referred to the right axis. Due to graphical reasons, the J values are divided by a factor of 10 in both panels, while τ is divided by a factor of 2 in panel (b) only.

Table 3. Best fit parameters corresponding to the fit of experimental data of both samples to equation (6) in the *clean limit* case. $\tilde{\chi}^2_{\rm min}$ indicates the absolute minimum of $\tilde{\chi}^2$, where $\tilde{\chi}^2 = \chi^2/\text{d.o.f.}$ and d.o.f. = 10 for sample WI3B_1 and d.o.f. = 9 for sample WI3C_1.

Sample	T_c (K)	$\tilde{\chi}^2_{\rm min}$	s (Å)	τ (10^{-14} s)	J (K)
WI3B_1	78.05 ± 0.22	0.14	$6.36^{+0.03}_{-0.23}$	$0.97^{+0.11}_{-0.02}$	17^{+11}_{-17}
WI3C_1	75.77 ± 0.38	0.56	$2.91^{+0.02}_{-0.17}$	$1.75^{+0.07}_{-0.02}$	21^{+17}_{-21}

same procedure as the fits to equation (6) in the *intermediate* case, which has been illustrated in figures 2 and 3.

In figure 4 the behaviours of $\tilde{\chi}^2$ as a function of T_c are reported for both samples. It is apparent that, also in this new approximation, well-defined minimum regions of $\tilde{\chi}^2$ exist with reasonable values of $\tilde{\chi}^2_{\rm min}$. Therefore, it was possible to apply the above-mentioned procedure for the estimation of the values of T_c and of the other parameters, along with their uncertainties. The results are displayed in table 3.

By comparing the $\tilde{\chi}^2_{\rm min}$ values reported in tables 2 and 3, it is clear that basically both approximations can account equally well for the experimental data. As far as s is concerned, the *clean limit* case induces an increase by a factor of 13–17 with respect to the *intermediate* case, which makes the resulting values quite similar to the d values obtained by the pure 2D AL law used for the preliminary estimation of T_c. In spite of the fact that such results are sample

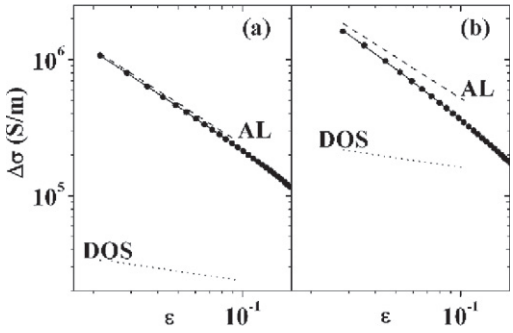

Figure 5. Best fits of the experimental data to equation (6) in the *clean limit* case for samples WI3B_1 (a) and WI3C_1 (b). Fits are represented by solid lines, single contributions by dashed and dotted lines, as indicated. The DOS term is plotted in absolute value. The corresponding parameter values are reported in table 3.

dependent and have no definite correspondence with the crystal structure, they are nearly identical to the values $s = 7$–8 Å reported by some authors for Bi-2212 [12, 44, 46, 47]. On the other hand, a decrease of a factor between 20 and 40 occurs for the values of the J parameter, so that the results corresponding to the *clean limit* case appear to be compatible with the ones from several previous studies on Bi-2212 [11, 12, 25, 27, 30, 34], on $(Tl, Hg)_2Ba_2Ca_2Cu_3O_{10+\delta}$ [10] and on $Tl_2Ba_2CaCu_2O_{8+y}$ [32] single crystals. Finally, it can be observed that, in the present approximation, τ increases by amounts of 46% and of 110% for samples WI3B_1 and WI3C_1, respectively, and consequently $4\pi\tau k_B T/\hbar = 2.4$ as the maximum value. This means that the erroneous assumption $4\pi\tau k_B T/\hbar \gg 1$ seems not too far from being satisfied in a self-consistent way when one fails to correctly try the *intermediate* case, due to a sort of self-enhancement effect.

The best fits corresponding to the parameter values listed in table 3 are reported in figure 5. They show that such combinations of the parameters result in a remarkable decrease of the importance of the DOS term with respect to the *intermediate* case: this contribution ranges between only 3% and 32% of the AL term for the two samples. This result clarifies that the form of the k coefficient plays a key role in determining the relative importance of the different processes involved in the paraconductivity and, along with the similarity between the s values of the *clean limit* case and the d values of the pure 2D AL law, shows that these two treatments are practically equivalent. Therefore, according to the present *non*-self-consistent approximation, it could be stated that the AL process is dominant and that the DOS term is only a minor correction, with no need of the Maki–Thompson process to explain the experimental data. Although this is the hierarchy commonly accepted among the various paraconductivity contributions, our analysis demonstrates that the hypotheses leading to such a conclusion are not justified in our experiment. In order to be self-consistent, one should return to the general *intermediate* case of equation (6), but this would generate unacceptable values of s.

On the basis of such an unsatisfactory situation, we were induced to reconsider the choice of excluding any role of the MT process in the interpretation of the data. Therefore we resorted to the full thermodynamical fluctuation theory described by equations (1)–(5), which means that τ_ϕ was restored as a free parameter because of the reintroduction of the anomalous Maki–Thompson term. The *intermediate* case of the theory was applied by means of the general procedure described above.

The contour plots of $\tilde{\chi}^2$ are shown in figure 6 for the investigated portions of the (s, T_c) plane. It is apparent that both samples show a wide minimum which is much more sensitive to the variations of T_c than of s.

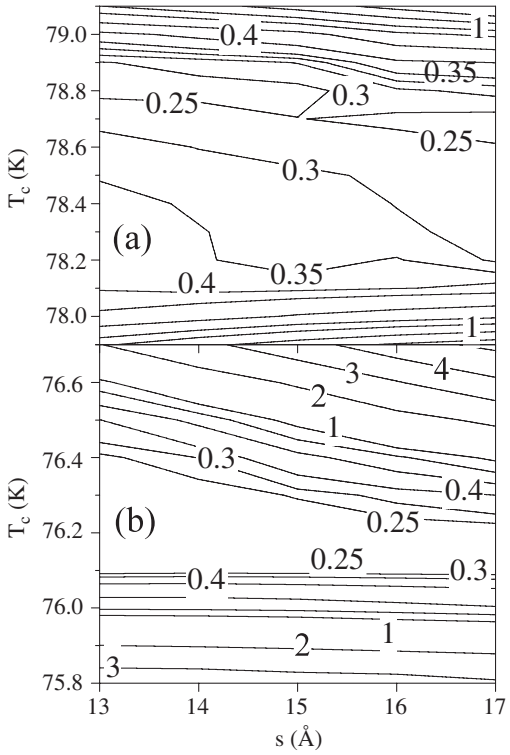

Figure 6. Contour plots of the reduced chi square $\tilde{\chi}^2 = \chi^2/\text{d.o.f.}$ in the (s, T_c) plane obtained by fitting the experimental data of samples WI3B_1 (a) and WI3C_1 (b) to equation (1) in the general *intermediate* case. d.o.f. = 18 for both samples. Contiguous lines are variably spaced.

Table 4. Best fit parameters deduced from fitting the experimental data of both samples to equation (1) in the general *intermediate* case by fixing $s = 15$ Å. $\tilde{\chi}^2_{\text{min}}$ indicates the absolute minimum of $\tilde{\chi}^2$, where $\tilde{\chi}^2 = \chi^2/\text{d.o.f.}$ and d.o.f. = 18 for both samples.

Sample	T_c (K)	$\tilde{\chi}^2_{\text{min}}$	τ_ϕ (10^{-12} s)	τ (10^{-14} s)	J (K)
WI3B_1	78.5 ± 0.4	0.23	$1.1^{+1.5}_{-0.3}$	$1.77^{+0.01}_{-0.04}$	35^{+25}_{-35}
WI3C_1	76.2 ± 0.1	0.20	3.0 ± 0.6	$2.77^{+0.03}_{-0.05}$	14^{+6}_{-14}

In figure 7 the contour plots are presented for the best fit values of τ_ϕ, τ and J. These results confirm the relatively low dependence on the value of s; the dependence on T_c is also rather weak for τ_ϕ and τ, while J shows much stronger variations. It is worth stressing that the fit results are very similar for both samples, which confirms the reliability of the analysis.

Since the structure of the results clearly shows that s has only a minor influence both on $\tilde{\chi}^2$ and on the values of the remaining parameters, it follows that it is not possible to select its best fit value in a reliable way by considering only the information coming from the minimization procedure. We therefore exploited the knowledge of the Bi-2212 structure provided by crystallographic studies and decided to fix $s = 15$ Å, as expected from the presence of two Cu–O bilayers per unit cell. The corresponding behaviours for all the relevant quantities are compared in figure 8 as a function of T_c.

The $\tilde{\chi}^2$ minimum regions can be clearly identified for both samples and show very reasonable values of $\tilde{\chi}^2_{\text{min}}$. Therefore, it was possible to apply the usual procedure for the

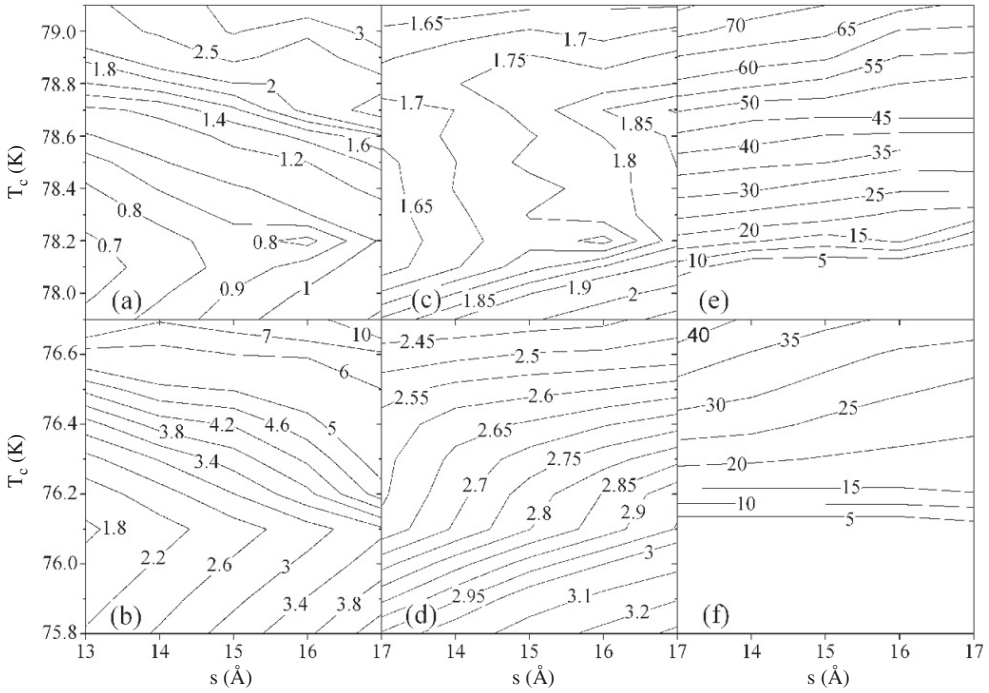

Figure 7. Contour plots of the phase-breaking time τ_ϕ (panels (a) and (b)), of the quasiparticle scattering time τ (panels (c) and (d)) and of the hopping energy between adjacent layers J (panels (e) and (f)) for the fits to equation (1) in the general *intermediate* case. Panels (a), (c) and (e) refer to sample WI3B_1, while panels (b), (d) and (f) correspond to sample WI3C_1. Labels are in units of 10^{-12} s for τ_ϕ, in units of 10^{-14} s for τ and in units of kelvin for J.

estimation of T_c, τ_ϕ, τ, J and their respective uncertainties. They are reported in table 4, while the best fits corresponding to the estimated parameters are shown in figure 9.

It is apparent that the theory fits the data of both samples excellently in the reduced temperature ranges $0.021 \leqslant \varepsilon \leqslant 0.148$ for sample WI3B_1 and $0.026 \leqslant \varepsilon \leqslant 0.155$ for sample WI3C_1, which are considerably larger than the validity ranges of the two previous descriptions without the MT terms.

Regarding the parameters, we note that the T_c values, even if slightly larger than the ones reported in tables 2 and 3, are both within the T_c ranges estimated in a preliminary way by means of the pure 2D AL law. We also observe that the values deduced for J and τ are fully consistent with previous studies for Bi-2212 [11, 12, 25, 27, 30, 34], while the τ_ϕ values are, to our knowledge, the largest ever reported for any HTSC compound [10–12, 22, 24–27, 29–32, 34]. Correspondingly, the anomalous MT terms exceed all the other contributions by at least a factor of 2 over the whole temperature range, which would call for a reassessment of the commonly accepted hierarchy.

Therefore, such a situation deserves some further analysis. It should be noted that τ_ϕ is a fundamental parameter of the weak localization theory [48] and, as such, it has been extensively studied both from a theoretical and from an experimental point of view in several different systems. At $T \geqslant 20$ K it is generally accepted that the electron–phonon interaction is by far the most important source of dephasing for each electron and the temperature dependence law most commonly observed in metals is $\tau_\phi \propto T^{-2}$ because of the interference between the electron–

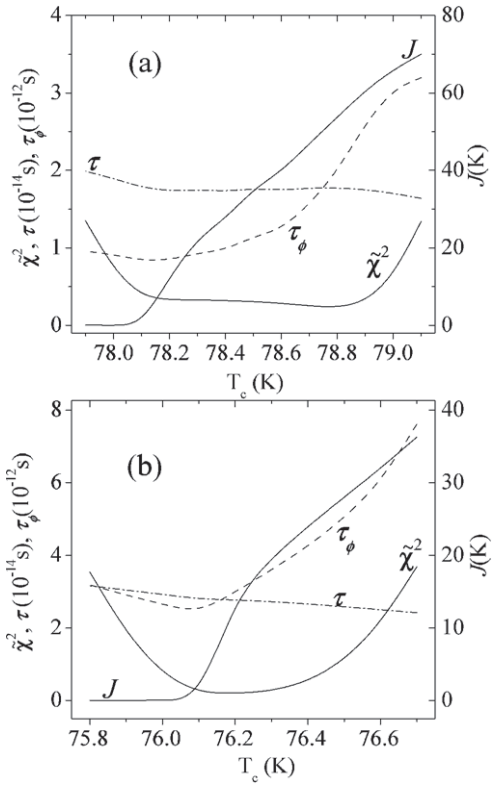

Figure 8. Behaviour of $\tilde{\chi}^2$ (——), τ_ϕ (- - - -), τ (— · —) and J (——) along the $s = 15$ Å section of the (s, T_c) plane for the fits of samples WI3B_1 (a) and WI3C_1 (b) to equation (1) in the general *intermediate* case. $\tilde{\chi}^2$, τ_ϕ, τ values are referred to the left axis, J is referred to the right axis.

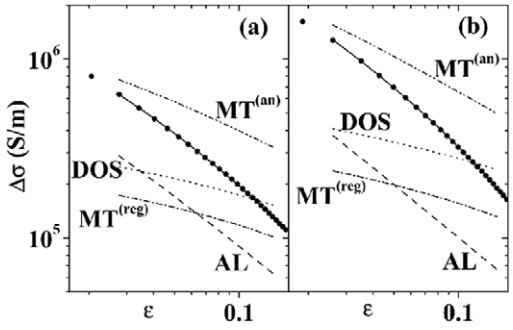

Figure 9. Best fits of the experimental data to equation (1) in the general *intermediate* case for samples WI3B_1 (a) and WI3C_1 (b). Fits are represented by solid lines, single contributions by dashed and dotted lines, as indicated. Negative terms (i.e. DOS and $MT^{(reg)}$) are plotted in absolute values. The corresponding parameter values are reported in table 4.

impurity and the electron–transverse phonon scattering [49, 50]. Electron–phonon scattering times $\tau_{e,ph} \approx \tau_\phi$ of the order of 10^{-13}–10^{-12} s at $T \approx 80$ K can be deduced from the high-temperature extrapolation of the theoretical law followed by the experimental results in many metallic systems, e.g. CuCr wires [51] and Al, Au, Mg, Nb, NbC and Be films [49, 50, 52–54].

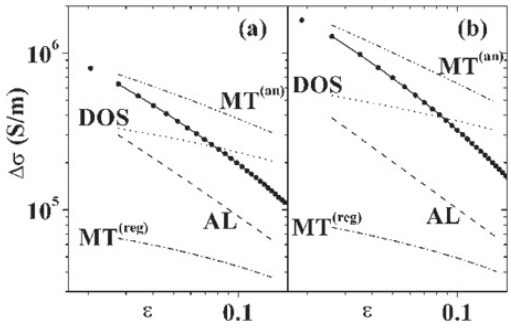

Figure 10. Best fits of the experimental data to equation (1) in the general *intermediate* case for samples WI3B_1 (a) and WI3C_1 (b), obtained by fixing $s = 15$ Å and the T_c values according to the results from table 4 and by using the definition of $\tilde{k}$ from [8]. Fits are represented by solid lines, single contributions by dashed and dotted lines, as indicated. Negative terms (i.e. DOS and $MT^{(reg)}$) are plotted in absolute values. The corresponding parameter values are reported in table 5.

Table 5. Best fit parameters corresponding to the fits of the experimental data of both samples to equation (1) in the general *intermediate* case, obtained by fixing $s = 15$ Å and the T_c values according to the results from table 4. Unlike table 4, the definition of $\tilde{k}$ follows [8]. $\tilde{\chi}^2 = \chi^2/\text{d.o.f.}$ and d.o.f. $= 18$ for both samples.

Sample	T_c (K)	$\tilde{\chi}^2$	τ_ϕ (10^{-12} s)	τ (10^{-14} s)	J (K)
WI3B_1	78.5	0.20	0.71	2.45	28
WI3C_1	76.2	0.33	1.86	3.58	6.8

On the other hand, several measurements of τ_ϕ have also been performed in semiconducting structures, where dephasing times of the same orders of magnitude can be inferred from the experiments in open InGaAs quantum dots [55] and in GaAs quantum wires [56]. Actually, a dephasing time as long as 11×10^{-12} s at $T = 75$ K has been measured in epitaxial InGaAs quantum dots [57], confirming that similar τ_ϕ values are possible for electron systems that are strongly confined in a multiple layer structure.

Remembering that the form of the k coefficient had already been shown to have great importance in determining the relative weight of the different contributions to the excess conductivity, we have suspected that a similar influence was held by the coefficient $\tilde{k}$ as well. Therefore we determined whether our new result could be due to the difference between the definition of $\tilde{k}$ used in the present paper and the slightly different one reported in [8]. Therefore, the fits were repeated under exactly the same conditions and using the same procedure (except for the definition of $\tilde{k}$) by using the T_c values listed in table 4. The parameter values corresponding to the best fits achievable according to this procedure are listed in table 5 and the corresponding fits are displayed in figure 10.

Table 5 shows that a τ_ϕ decrease by 38% was observed in both samples in comparison with the results listed in table 4, together with an increase of τ (29–38%) and a decrease of J (20–50%). However, figure 10 clarifies that these changes were not large enough to significantly modify the new hierarchy among the contributions: the anomalous MT terms were only slightly reduced (<5%), the AL terms increased by less than 4% and the DOS term increase, even if important (32–35%), did not allow it to equal the anomalous MT contribution. The most important effect in using the formula of [8] was the reduction of the regular MT terms, which were depressed by 62–69%, as expected both from the additional 1/2 factor and from the

increase of τ in the $\psi''(1/2)$ coefficient of $\tilde{k}$. The fits reported in figure 10 show that almost all of this reduction was counterbalanced by the only other negative term, i.e. the DOS term, which increased accordingly. This allowed us to conclude that the correction in the definition of the coefficient $\tilde{k}$ seems to play only a minor role in our results.

In order to acquire further confidence in our analysis, we cross-checked its implications by computing $\xi_c(0) = s\sqrt{r(T_c)}/2$ and obtained $\xi_c(0) = 0.8$ Å and $\xi_c(0) = 0.4$ Å for samples WI3B_1 and WI3C_1, respectively. Such values are in general agreement with previous experiments on Bi-2212 [16, 18, 19, 58]. Also the Fermi level E_F can be estimated in the Drude framework from ρ_a^n and the microscopic parameters via the formula $E_F = \hbar^2\pi s/(e^2\tau\rho_a^n)$. This gives 0.71 and 0.54 eV for samples WI3B_1 and WI3C_1, respectively, which have to be considered as upper limits of the real values, because of the assumption of a cylindrical Fermi surface underlying the theory. These energies are fairly similar to those obtained by a previous analysis of the same kind performed on thin films [27] and agree well with the band structure calculated from first principles for Bi-2212 [59]. Moreover, the same framework provides carrier densities $n = m^*/(e^2\tau\rho_a^n)$ about 1.5–1.9 $\times 10^{21}$ cm^{-3} for the two samples, if the free electron mass is assumed for the effective carrier mass m^*. This estimate lies in the same range of a determination by chemical methods [60] and within a factor of 2–3 from the results obtained by Hall coefficient measurements [61–63].

Moreover, the results listed in table 2 imply that $4\pi\tau k_B T/\hbar = 2.3$–$4.0$, confirming that the clean limit $4\pi\tau k_B T/\hbar \gg 1$ is not fully reached for these crystals. We also note that $\tau_\phi/\tau \approx 60$–$110$, therefore fulfilling the requirement $\tau_\phi > \tau$ for the inelastic versus elastic scattering and showing that about one hundred scattering events are required before the MT pairs are decoupled. The comparison between the phase-breaking γ_ϕ and the anisotropy r parameters shows that $\gamma_\phi/r \approx 1.2$–$1.8$ and therefore neither the weak ($\ll 1$) nor the strong ($\gg 1$) limit can be considered for the phase-breaking intensity. We obtain for the interlayer tunnelling rates $J^2\tau/\hbar^2 \approx 0.9$–$3.7 \times 10^{11}$ s^{-1} and for the phase-breaking rates $\tau_\phi^{-1} \approx 3.3$–$8.7 \times 10^{11}$ s^{-1}. Therefore, the ratio between the two rates, $\tau_\phi^{-1}/(J^2\tau/\hbar^2)$, is about 2.3–3.6, so that the condition for incoherent tunnelling along the c-axis ($\tau_\phi^{-1}/(J^2\tau/\hbar^2) > 1$) holds, although only marginally. Consequently, Josephson effect precursor phenomena cannot be excluded *a priori* in similar systems. Finally, we note that these results, by asserting that the MT contribution is far from vanishing, imply that the s-wave symmetry should be an important component of the order parameter for $T \gtrsim T_c$ [9, 28]. This is the same conclusion already reached for $T \leqslant T_c$ by recent experiments on the c-axis Josephson tunnelling across twisted Bi-2212 bicrystals [64] and on angle-resolved in-plane electron tunnelling for untwinned YBCO films [65]. Furthermore, our observation of a marginally incoherent tunnelling in the c-axis direction could support Klemm's interpretation [66] of another twist tunnelling experiment in overdoped Bi-2212 whiskers, according to which the results by Takano *et al* [67] are consistent with an s-wave symmetry accompanied by an intrinsically coherent c-axis tunnelling and a hot-spot Fermi surface.

4. Conclusions

The high quality of the experimental data and the very careful fitting procedure has allowed us to show that the MT process may be an important contribution to the excess conductivity originating from the superconducting fluctuations above T_c in crystals with micrometric transverse sizes and that the microscopic parameters of the material can be reliably extracted from the analysis of the paraconductivity. The lack of self-consistency in more traditional alternative interpretations has also been illustrated. Because of the novelty of the results of our

analysis, it would perhaps be useful to perform new paraconductivity experiments in non-zero magnetic field on high-quality freshly grown crystals. Nevertheless our conclusions give an indication for an important s-wave symmetry component in the order parameter of Bi-2212 at $T \gtrsim T_c$.

Acknowledgments

This work was partly supported by INFM under project PAIS-STRIPES. We would like to acknowledge C Manfredotti, E Vittone, A Lo Giudice, E Silva, R Fastampa, S Sarti, R Gonnelli and A Werbrouck for useful discussions. We give special thanks to A Varlamov for his valuable help and to A Causio, C Paolini and P Olivero for their contribution in the preliminary part of the work.

References

[1] Aslamazov L G and Larkin A I 1968 The influence of fluctuation pairing of electrons on the conductivity of normal metal *Phys. Lett.* A **26** 238–9
[2] Maki K 1968 Critical fluctuation of the order parameter in a superconductor. I *Prog. Theor. Phys.* **40** 193–200
[3] Thompson R S 1970 Microwave, flux flow, and fluctuation resistance of dirty type-II superconductors *Phys. Rev.* B **1** 327–33
[4] Skocpol W J and Tinkham M 1975 Fluctuations near superconducting phase transitions *Rep. Prog. Phys.* **38** 1049–97
[5] Freitas P P, Tsuei C C and Plaskett T S 1987 Thermodynamic fluctuations in the superconductor $Y_1Ba_2Cu_3O_{9-\delta}$: evidence for three dimensional superconductivity *Phys. Rev.* B **36** 833–5
[6] Lawrence W E and Doniach S 1971 *Proc. 12th Int. Conf. on Low Temperature Physics (Kyoto, 1970)* ed E Kanda, pp 361–2
[7] Dorin V V, Klemm R A, Varlamov A A, Budzin A I and Livanov D V 1993 Fluctuation conductivity of layered superconductors in a perpendicular magnetic field *Phys. Rev.* B **48** 12951–65
[8] Varlamov A A, Balestrino G, Milani E and Livanov D V 1999 The role of density of states fluctuations in the normal state properties of high T_c superconductors *Adv. Phys.* **48** 655–783
[9] Larkin A I and Varlamov A A 2005 *Theory of Fluctuations in Superconductors* (*International Series of Monographs on Physics* vol 127) 1st edn (New York: Oxford University Press)
[10] Wahl A, Thopart D, Villard G, Maignan A, Hardy V, Soret J C, Ammor L and Ruyter A 1999 *c*-axis magnetoconductivity of anisotropic superconducting single crystals: the density-of-states fluctuation scenario *Phys. Rev.* B **59** 7216–21
[11] Wahl A, Thopart D, Villard G, Maignan A, Simon Ch, Soret J C, Ammor L and Ruyter A 1999 Magnetotransport in $Bi_2Sr_2Ca_{1-x}Y_xCu_2O_{8+\delta}$ single crystals: from the underdoped to the overdoped regime *Phys. Rev.* B **60** 12495–501
[12] Balestrino G, Crisan A, Livanov D V, Manokhin S I and Milani E 2001 Fluctuation magnetoconductivity of BSCCO-2212 films in parallel magnetic field *Physica* C **355** 135–9
[13] Ausloos M and Laurent C 1988 Thermodynamic fluctuations in the superconductor $Y_1Ba_2Cu_2O_{9-y}$: evidence for two-dimensional superconductivity *Phys. Rev.* B **37** 611–4
[14] Cimberle M R, Ferdeghini C, Giannini E, Marré D, Putti M, Siri A, Federici F and Varlamov A 1997 Crossover between Aslamazov–Larkin and short-wavelength fluctuation regimes in high-temperature-superconductors conductivity experiments *Phys. Rev.* B **55** R14745–8
[15] Höpfengartner R, Hensel B and Saemann-Ischenko G 1991 Analysis of the fluctuation-induced excess dc conductivity of epitaxial $YBa_2Cu_3O_7$ films: influence of a short-wavelength cutoff in the fluctuation spectrum *Phys. Rev.* B **44** 741–9
[16] Mun M-O, Lee S-I, Suck Salk S-H, Shin H J and Joo M K 1993 Conductivity fluctuations in a single crystal of $Bi_2Sr_2CaCu_2O_x$ *Phys. Rev.* B **48** 6703–6
[17] Pradhan A K, Roy S B, Chaddah P, Chen C and Wanklyn B M 1994 Fluctuation phenomena in excess conductivity and magnetization of single-crystal $Bi_2Sr_2CaCu_2O_{8+y}$ *Phys. Rev.* B **50** 7180–3
[18] Pomar A, Ramallo M V, Mosqueira J, Torrón C and Vidal F 1996 Fluctuation-induced in-plane conductivity, magnetoconductivity, and diamagnetism of $Bi_2Sr_2CaCu_2O_8$ single crystals in weak magnetic fields *Phys. Rev.* B **54** 7470–80

[19] Han S H, Zhao Y, Gu G D, Russell G J and Koshizuka N 1997 In-plane paraconductivity of $Bi_2Sr_2CaCu_2O_8$ single crystals with different resistivity anisotropies *Phys. Status Solidi* b **203** 189–94
[20] Han S H, Eltsev Yu and Rapp Ö 1998 Resistive transition and fluctuation conductivity in $Bi_2Sr_2CaCu_2O_{8+\delta}$ single crystals *Phys. Rev.* B **57** 7510–3
[21] Enomoto H, Mori N, Matsubara I and Ozaki H 2000 Paraconductivity analysis for superconducting Bi-Sr-Ca-Cu-O whiskers *Physica* B **284–288** 579–80
[22] Latyshev Yu I, Laborde O and Monceau P 1995 The normal-state magnetoresistance of BSCCO 2:2:1:2 single-crystal whiskers *Europhys. Lett.* **29** 495–500
[23] Livanov D V, Milani E, Balestrino G and Aruta C 1997 In-plane and out-of-plane transport properties of $Bi_2Sr_2CaCu_2O_{8+x}$ epitaxial films: fluctuations and transition into a vortex solid state *Phys. Rev.* B **55** R8701–4
[24] Semba K and Matsuda A 1997 Vanishing small Maki–Thompson superconducting fluctuation in the magnetoresistance of high-T_c superconductors *Phys. Rev.* B **55** 11103–6
[25] Heine G, Lang W, Wang X L and Dou S X 1999 Positive in-plane and negative out-of-plane magnetoresistance in the overdoped high-temperature superconductor $Bi_2Sr_2CaCu_2O_{8+x}$ *Phys. Rev.* B **59** 11179–82
[26] Holm W, Rapp Ö, Johnson C N L and Helmersson U 1995 Magnetoconductivity in $YBa_2Cu_3O_{7-\delta}$ thin films *Phys. Rev.* B **52** 3748–55
[27] Nygmatulin A S, Varlamov A A, Livanov D V, Balestrino G and Milani E 1996 Effect of the magnetic field on the *c*-axis resistance peak in $Bi_2Sr_2CaCu_2O_{8+x}$ epitaxial films *Phys. Rev.* B **53** 3557–60
[28] Carretta P, Livanov D V, Rigamonti A and Varlamov A A 1996 Superconducting fluctuations and ^{63}Cu NQR-NMR relaxation in $YBa_2Cu_3O_{7-\delta}$: effect of magnetic field and a test for the pairing-state symmetry *Phys. Rev.* B **54** R9682–5
[29] Axnäs J, Lundqvist B and Rapp Ö 1998 High-temperature magnetoconductivity of $YBa_2Cu_3O_{7-\delta}$: reconsideration of the Maki–Thompson contribution *Phys. Rev.* B **58** 6628–32
[30] Thopart D, Wahl A, Warmont F, Simon Ch, Soret J C, Ammor L, Ruyter A, Buzdin A I, Varlamov A A and de Brion S 2000 Relevance of the scheme of regularization of the density-of-state fluctuation contribution in an arbitrary magnetic field *Phys. Rev.* B **62** 9721–5
[31] Bjornängen T, Axnäs J, Eltsev Yu, Rydh A and Rapp Ö 2001 In-plane anisotropy and possible chain contribution to magnetoconductivity in $YBa_2Cu_3O_{7-\delta}$ *Phys. Rev.* B **63** 224518
[32] Kim H-J, Chowdhury P, Kang W N, Zang D-J and Lee S-I 2003 Superconducting fluctuation probed by in-plane and out-of-plane conductivities in $Tl_2Ba_2CaCu_2O_{8+y}$ single crystals *Phys. Rev.* B **67** 144502
[33] Kim H-J, Chowdhury P, Gupta S K, Dan N H and Lee S-I 2004 Effect of thermodynamic fluctuations on in-plane and out-of-plane magnetoresistance of monolayer superconductor $Tl_2Ba_2CuO_{6+\delta}$ *Phys. Rev.* B **70** 144510
[34] Chowdhury P and Bhatia S N 1999 Effect of reduction in the density of states on fluctuation conductivity in $Bi_2Sr_2CaCu_2O_{8+x}$ single crystals *Physica* C **319** 150–8
[35] Gorlova I G and Timofeev V N 1995 The crystal structure and excess conductivity of BSCCO (2212) whiskers *Physica* C **255** 131–5
[36] Timofeev V N and Gorlova I G 1998 Growth defects in BSCCO (2212) single crystal whiskers *Physica* C **309** 113–9
[37] Li T W, Kes P H, Fu W T, Menovsky A A and Franse J J M 1994 Anisotropic oxygen diffusion in $Bi_2Sr_2CaCu_2O_{8+x}$ single crystals *Physica* C **224** 110–6
[38] Truccato M, Lamberti C, Prestipino C and Agostino A 2005 Evidence of ion diffusion at room temperature in microcrystals of the $Bi_2Sr_2CaCu_2O_{8+\delta}$ superconductor *Appl. Phys. Lett.* **86** 213116
[39] Truccato M, Rinaudo G, Manfredotti C, Agostino A, Benzi P, Volpe P, Paolini C and Olivero P 2002 Growth, contacting and ageing of superconducting Bi-2212 whiskers *Supercond. Sci. Technol.* **15** 1304–10
[40] Esposito M, Muzzi L, Sarti S, Fastampa R and Silva E 2000 Determination of the resistivity components ρ_{ab} and ρ_c from $Bi_2Sr_2CaCu_2O_x$ crystals *J. Appl. Phys.* **88** 2724–9
[41] Silva E, Sarti S, Fastampa R and Giura M 2001 Excess conductivity of overdoped $Bi_2Sr_2CaCu_2O_{8+\delta}$ crystals well above T_c *Phys. Rev.* B **64** 144508
[42] Stupp S E, Lee W C, Giapintzakis J and Ginsberg D M 1992 Constraints on the temperature dependence of the magnetic penetration depth of superconducting $Bi_2Sr_2CaCu_2O_{8+x}$ from measurements of the low-temperature specific heat *Phys. Rev.* B **45** 3093–7
[43] Meingast C, Junod A and Walker E 1996 Superconducting fluctuations and uniaxial-pressure dependence of T_c of a $Bi_2Sr_2CaCu_2O_{8+x}$ single crystal from high-resolution thermal expansion *Physica* C **272** 106–14
[44] Latyshev Y I, Gorlova I G, Nikitina A M, Antokhina V U, Zybtsev S G, Kukhta N P and Timofeev V N 1993 Growth and study of single-phase 2212 BSCCO whiskers of submicron cross-sectional area *Physica* C **216** 471–7

[45] Balestrino G, Marinelli M, Milani E, Reggiani L, Vaglio R and Varlamov A A 1992 Excess conductivity in 2:2:1:2-phase Bi-Sr-Ca-Cu-O epitaxial thin films *Phys. Rev.* B **46** 14919–21
[46] Gorlova I G, Zybtsev S G, Pokrovskii V Ya and Timofeev V N 1997 Fluctuation phenomena in BSCCO(2212) whiskers *Fluctuation Phenomena in High Temperature Superconductors* ed M Ausloos and A A Varlamov (Dordrecht: Kluwer–Academic) pp 113–20
[47] Gorlova I G, Zybtsev S G, Pokrovskii V Ya and Timofeev V N 1997 Fluctuation of BSCCO(2212) whiskers *Physica* C **282–287** 1533–4
[48] Washburn S and Webb R A 1992 Quantum transport in small disordered samples from the diffusive to the ballistic regime *Rep. Prog. Phys.* **55** 1311–83
[49] Sergeev A and Mitin V 2000 Electron–phonon interaction in disordered conductors: static and vibrating scattering potentials *Phys. Rev.* B **61** 6041–7
[50] Ptitsina N G, Chulkova G M, Il'in K S, Sergeev A V, Pochinkov F S, Gershenzon E M and Gershenson M E 1997 Electron–phonon interaction in disordered metal films: the resistivity and electron dephasing rate *Phys. Rev.* B **56** 10089–96
[51] DiTusa J F, Lin K, Park M, Isaacson M S and Parpia J M 1992 Role of phonon dimensionality on electron–phonon scattering rates *Phys. Rev. Lett.* **68** 1156–9
[52] Bergmann G 1984 Quantum corrections to the resistance in two-dimensional disordered superconductors above T_c: Al, Sn and amorphous $Bi_{0.9}Tl_{0.1}$ films *Phys. Rev.* B **29** 6114–28
[53] Bergmann G 1983 Consistent temperature and field dependence in weak localization *Phys. Rev.* B **28** 515–22
[54] Belitz D and Das Sarma S 1987 Inelastic phase-coherence time in thin metal films *Phys. Rev.* B **36** 7701–4
[55] Hackens B, Delfosse F, Faniel S, Gustin C, Boutry H, Wallart X, Huynen I, Bollaert S, Cappy A and Bayot V 2002 Long dephasing time and high temperature conductance fluctuations in an InGaAs open quantum dot *Phys. Rev.* B **66** 241305
[56] Hiramoto T, Hirakawa K, Iye Y and Ikoma T 1989 Phase coherence length of electron waves in narrow AlGaAs/GaAs quantum wires fabricated by focused ion beam implantation *Appl. Phys. Lett.* **54** 2103–5
[57] Mohanty P, Jariwala E M Q and Webb R A 1997 Intrisic decoherence in mesoscopic systems *Phys. Rev. Lett.* **78** 3366–9
[58] Palstra T T M, Batlogg B, Schneemeyer L F, van Dover R B and Waszczak J V 1988 Angular dependence of the upper critical field of $Bi_{2.2}Sr_2Ca_{0.8}Cu_2O_{8+\delta}$ *Phys. Rev.* B **38** 5102–5
[59] Bellini V, Ambrosch-Draxl C and Manghi F 2003 First-principles study of the normal state electronic properties of the Bi-2212 cuprate superconductor *Mater. Sci. Eng.* C **23** 885–8
[60] Idemoto Y, Toda T and Fueki K 1995 Comparison of Bi-rich and Cu-rich oxides of the Bi-2212 phase *Physica* C **249** 123–32
[61] Hopfengärtner R, Leghissa M, Kreiselmeyer G, Holzapfel B, Schmitt P and Saemann-Ischenko G 1993 Hall effect of epitaxial $YBa_2Cu_3O_{7-x}$ and $Bi_2Sr_2CaCu_2O_y$ films: interpretation of the Hall effect on the basis of a renormalized tight-binding model *Phys. Rev.* B **47** 5992–6003
[62] Iye Y, Nakamura S and Tamegai T 1989 Hall effect in high temperature superconductors near T_c *Physica* C **159** 616–24
[63] Maeda A, Noda K, Takebayashi S and Uchinokura K 1989 Preparation and physical properties of $Bi_2Sr_2Ca_{n-1}Cu_nO_y$ *Physica* C **162–164** 1205–6
[64] Li Qiang, Tsay Y N, Suenaga M, Klemm R A, Gu G D and Koshizuka N 1999 $Bi_2Sr_2CaCu_2O_{8+\delta}$ bicrystal c-axis twist Josephson junctions: a new phase-sensitive test of order parameter symmetry *Phys. Rev. Lett.* **83** 4160–3
[65] Smilde H J H, Golubov A A, Ariando, Rijnders G, Dekkers J M, Harkema S, Blank D H A, Rogalla H and Hilgenkamp H 2005 Admixtures to d-wave gap symmetry in untwinned $YBa_2Cu_3O_7$ superconducting films measured by angle-resolved electron tunneling *Phys. Rev. Lett.* **95** 257001
[66] Klemm R A 2003 Theory of $Bi_2Sr_2CaCu_2O_{8+\delta}$ cross-whisker Josephson junctions *Phys. Rev.* B **67** 174509
[67] Takano Y, Hatano T, Fukuyo A, Ishii A, Ohmori M, Arisawa S, Togano K and Tachiki M 2002 d-like symmetry of the order parameter and intrinsic Josephson effects in $Bi_2Sr_2CaCu_2O_{8+\delta}$ cross-whisker junctions *Phys. Rev.* B **65** 140513